HHS Public Access

Author manuscript

Ann N Y Acad Sci. Author manuscript; available in PMC 2016 August 26.

Published in final edited form as:

Ann N Y Acad Sci. 2009 May ; 1164: 89–96. doi:10.1111/j.1749-6632.2009.03845.x.

Effect of Canal Plugging on Quadrupedal Locomotion in Monkey

Bernard Cohen[a], **Yongqing Xiang**[b], **Sergei B. Yakushin**[a], **Mikhail Kunin**[b], **Theodore Raphan**[b], **Lloyd Minor**[c], and **Charles C. Della Santina**[c]

[a]Department of Neurology, Mount Sinai School of Medicine, New York, New York 10029, USA

[b]Department of Computer & Information Science, Brooklyn College, City University of New York, New York, New York 11210, USA

[c]Department of Otolaryngology-Head & Neck Surgery, Johns Hopkins University, Baltimore, Maryland 21287, USA

Abstract

The vestibular system plays an important role in controling gait, but where in the labyrinths relevant activity arises is largely unknown. After the semicircular canals are plugged, low frequency (0.01–2 Hz) components of the angular vestibulo-ocular reflex (aVOR) and angular vestibulo-collic reflex (aVCR) are lost, but high frequency (3–20 Hz) components remain. We determined how loss of low frequency canal afference affects limb and head movements during quadrupedal locomotion. Head, body, and limb movements were recorded in three dimensions (3-D) in a cynomolgus monkey with a motion detection system, while the animal walked on a treadmill. All six canals were plugged, reducing the canal time constants from ≈4.0 sec to ≈0.07 sec. Major changes in the control of the limbs occurred after surgery. Fore and hind limbs were held farther from the body, producing a broad-based gait. Swing-phase trajectories were inaccurate, and control of medial-lateral limb movement was erratic. These changes in gait were present immediately after surgery, as well as 15 months later, when the animal had essentially recovered. Thus, control of the limbs in the horizontal plane was defective after loss of the low-frequency semicircular canal input and never recovered. Cycle-averaged pitch and roll head rotations, and 3-D head translations were also significantly larger and more erratic after than before surgery. Head rotations in yaw could not be quantified due to intrusion of voluntary head turns. These findings indicate that the semicircular canals provide critical low frequency information to maximize the accuracy of stepping and stabilize the head during normal quadrupedal locomotion.

Keywords

walking; semicircular canals; angular vestibulo-collic reflex (aVCR); vestibular; cynomolgus; swing-phase dynamics

Address for correspondence: Bernard Cohen, M.D., Department of Neurology, Box 1135, Mount Sinai School of Medicine, 1 East 100th Street New York, NY 10029-6574. Voice: +212-241-7068; fax: +212-831-1610. bernard.cohen@mssm.edu.

Conflicts of Interest

The authors declare no conflicts of interest.

Introduction

The vestibular system has a major role in stabilizing balance during locomotion, but the exact way in which this is accomplished is still a matter of conjecture, particularly during quadrupedal gait. It has been shown that lateral stability in roll and in the fore–aft direction are separately controlled during standing.[1,2] It has also been shown that postural stability is weaker in roll than in pitch,[3,4] and that lateral postural stability is reduced more than fore–aft stability in bilateral labyrinthine defective subjects and after unilateral labyrinthine lesions.[5] Where in the labyrinth activity responsible for such postural and locomotor stabilization arises and the characteristics of such activity are not known, particularly since labyrinthine lesions can affect both the semicircular canals and the otolith organs.

Plugging the semicircular canals has been an investigative tool since Ewald's pioneering studies in which he investigated the dynamics of the semicircular canals of pigeons after plugging the canals with gutta percha.[6] The resting discharge is maintained in the canal nerves after canal plugging,[7] however, indicating that changes in function are not of neural origin. More recently, using the angular vestibulo-ocular reflex (aVOR) as a test system, Yakushin and colleagues demonstrated that plugging the canals in monkeys primarily changed the dynamics of the cupula/endolymph system, reducing its time constant from a normal value of 3.5–4.5 sec to about 70 msec.[8] Rabbitt and colleagues[9] and Hess and colleagues[10] have come to the same conclusion. The consequence is that the low- and mid-band frequency responses of canal afferents (0.01 to 2 Hz) are lost after the semicircular canals are plugged, but high frequency input (3–20 Hz) is maintained. Since the canals also provide afferent input to the angular vestibulo-collic reflex (aVCR), the same is undoubtedly true of the aVCR. That is, only high frequency components are available to drive compensatory head movements after the canals are plugged. Thus, canal plugging can provide a quantitative tool for studying the effects of removal of low-frequency information from the sensors of head rotation, that is, the semicircular canals, but otherwise maintaining the input of the canals and otolith organs to the central vestibular system.

We have recently characterized the kinematics and dynamics of normal locomotion of monkeys walking on a treadmill[10] and have shown that the monkeys maintain relative stability of their heads during unrestrained quadrupedal gait.[11] In the latter study, angular head movements ranged between 5° and 10°, and head translations were small in all directions (≈2–4 cm). Most likely, this compensatory head stabilization originated largely in the aVCR. Here, we utilized the frequency filtering of canal plugging to investigate how a reduction in the low-frequency components of the afferent input from the semicircular canals would affect the kinematics and dynamics of stabilization of the head and limbs during quadrupedal walking.

Methods

A cynomolgus monkey (*Macaca fascicularis* Cy115) was trained to walk on a treadmill wearing rigid bodies that measured the three-dimensional position of its head, body, and limbs in space. The experiments conformed to the *Guide for the Care and Use of Laboratory Animal* experiments and were approved by the Institutional Animal Care and Use

Committee of the Mount Sinai School of Medicine. This report details the results of two test sessions, approximately 20 days after surgery (5/10/06 and 5/11/06; surgery was on 4/20/06), and compares them with two sessions recorded prior to surgery (10/28/05 and 11/03/05). We also recorded locomotion of Cy115 15 months after surgery (7/19/07).

Complete details of the Methods have been given in previous publications.[8,11,12] In brief, the animal was prepared under anesthesia and sterile surgical conditions with a head mount. This head mount held a cap with light emitting diodes (LEDs) that determined the spatial coordinates of the animal's head precisely in three dimensions while it was walking (Fig. 1A). A light body suit in this experiment held a rigid body on the postero-lateral chest wall. Small rigid bodies were fixed on tapes wrapped around the right wrist and right and left ankles (right forelimb, RFL; right hindlimb, RHL; and left hindlimb, LHL, Fig. 1A). After calibration, the angular and linear position of the rigid bodies could be detected with precision in three angular and linear dimensions as the animal walked relatively naturally on the treadmill, restrained only by a light chain.

Canal plugging was accomplished using techniques described previously.[8] Characteristics of aVOR gains were determined from scleral search coil recordings using passive rotation before and after operation. From the model of the effects of canal plugging,[8] the canal time constant was estimated to be ≈0.07 sec after operation, effectively limiting the canal-afferent frequency range to 3–20 Hz. Three Hz is above the stride frequencies, but below the step frequencies during normal quadrupedal walking.[11] Therefore, angular head movements associated with locomotion that fell below frequencies of 2–3 Hz would be decrementally sensed by the semicircular canals after operation.

Coordinate Frames, Data Collection, and Data Analysis

The inertial space–fixed coordinate frame (X, Y, Z) defined the origin of all other coordinate frames and the X–Z (vertical), X–Y (horizontal), and Y–Z (roll) planes (Fig. 1A). The Z axis was along the spatial vertical (positive upward), the positive X axis was along the direction of forward walking and orthogonal to the Z axis, and the Y axis was orthogonal to the X–Z plane, positive to the monkey's left. Rigid bodies on the head, the right thoracic wall, the RFL, and the RHL defined the positions of the head, body, and limbs in space. Head rotation relative to space was given in Euler angles in a Fick sequence (yaw, pitch, roll).

Movements of the head, right posterior chest wall (body), right wrist, and right ankle were detected by tracking the position of the infrared LEDs with a video-based motion detection system (Optotrak 3020, Northern Digital Inc., Canada). Optotrak data, sampled at 90~100 frames/sec, established the 3-D angular and linear positions of the rigid bodies on the trunk and limbs. A five-point average window filtered the data. Digital video of the monkey was recorded simultaneously with the locomotion data to help choose the cycles for analysis. Individual kinematic waveforms were averaged over limb stride cycles first, and parameters were derived from the averaged cycle. Approximately 10–15 cycles of gait were used for each condition at each walking velocity to characterize the frequencies, amplitudes, and phases of the translations and rotations of the head and body in pitch, yaw, and roll. The head and body in space were considered as rigid bodies that rotated and translated. Translational velocities and accelerations were determined by finding the slope of the linear

regression of 11 data points. Rotation matrices of the head and body were determined from the Optotrak data, and the axis and angle of the rotation were determined using the Euler-Rodriguez formula.[13,14] The components of the angular velocity vector along the X, Y, and Z axes were denoted as roll, pitch, and yaw velocities, respectively.

Results

Kinematics and dynamics of limb movement of juvenile macaque monkeys during quadrupedal walking have recently been characterized.[11] Cynomolgus monkeys typically walk with a diagonal gait sequence (Fig. 1A), in which the fore and hindlimbs on the same side move reciprocally along the X-axis. Typical swing phases of the RHL of Cy115 before all six canals were plugged are shown in Figure 1B. During representative gait cycles, the animal's hindlimb traveled forward ≈25 cm in space during the swing phases, and moved back in space during the stance phases, while the foot was planted on the belt of the treadmill (Fig. 1B). Lateral movement components were small along the Y-axis (Fig. 1C).

The X-axis limb movement had a unique pattern in that ankle velocity rose almost linearly to a maximum during the swing phases (≈1.5 m/sec) before dropping quickly to zero at the end of the swing. The limb then maintained a steady negative velocity during the stance phase (Fig. 1D). Deviations of limb velocity from linearity during the stance phases were due to the fact that the rigid body was on the ankle, which extended as the foot moved back. The hindlimb of the animal also moved slightly to the right, and then returned to the left at the end of the swing phases (Fig. 1C). Consistent with the small Y-axis movements, the lateral velocity was less than ≈0.5 m/s (Fig. 1E). These data confirmed that Cy115 had a typical gait and gait dynamics before surgery during quadrupedal walking.

The RFL and RHL had consistent oval-like patterns during the swing and stance phases when viewed from the side in the X–Z plane (Fig. 2A) or from above in the X–Y plane (Fig. 2C). The RHL swing phases, which began at the open circles, were chosen to synchronize the movements of the RFL and head and body. The limbs, body, and head then progressed along their average paths, shown by the heavy curved lines. Progressive darkening of the circles depicts the progression of the limbs, head, and body through the swing and stance phases of the RHL. Both the RHL and RFL had precise onsets and endpoints associated with the swing phases. The eccentricity of the oval-like trajectories of the RFL was small when viewed both from the side (Fig. 2A) and from above (Fig. 2C). Consistent with the theory of hindlimbs "driving" and the forelimbs "steering,"[15] the forelimbs were held farther from the body than the hindlimbs, and the eccentricity of their trajectories was smaller than those of the hindlimbs (Fig. 2C). Pacing was regular, and there was little forward (X) or upward (Z) movement of the head or body during these cycles (Fig. 2A,C). Viewed from above, the hindlimb trajectories were just lateral to the rigid body on the chest wall, while the linear forelimb trajectories were located about 6 cm from the chest rigid body.

Canal Plugging

By ≈3 wks after surgery, Cy115 had recovered from the acute effects of operation. Optotrak traces of the head, body, right hindlimb (RHL), and right forelimb (RFL) from the side (X–Z plane) and top (X–Y plane), before (Fig. 2A,C), and ≈3 wks after canal plugging (Fig.

2B,D) demonstrate the changes in gait produced by canal plugging. There were relatively few differences in either the stance or swing-phase trajectories when viewed from the side in the X–Z plane before (Fig. 2A) or after surgery (Fig. 2B). There were striking changes, however, in limb movement when viewed from the top in the X–Z plane (Fig. 2C,D). Both the fore and hind limbs were held farther from the body after surgery (compare vertical arrows, Fig. 2C,D), and their trajectories varied significantly from stride to stride. The lateral excursion of the swing phases in both fore and hind limbs had more than doubled after canal plugging, and variations in swing width were close to twice those before operation (Table 1).

Head movements were also affected, and the head made larger lateral swings with each step. Peak-to-peak amplitudes of head movements increased significantly in all translational and rotational directions except yaw (Table 2).

To compare swing phase trajectories in the X–Y plane, the starting points of the swing were translated to their mean value and overlaid (Fig. 3). Before surgery, the limbs moved predominantly in the forward–backward direction. There was slight curvature of the hindlimb movement, but the limb ended the swing phases within 2 cm of their initiation (Fig. 3A). The pre-operative swing phases of the forelimb were more precise—the limb moved directly ahead along the X-axis in the swing phases with little Y-axis movement (Fig. 3B). After surgery, Y-axis movement began at the onset of the swing phases (compare the shapes of the starting points), and the trajectories were spread laterally and medially, more in the forelimb (Fig. 3D) than in the hindlimb (Fig. 3C). These changes were long lasting, and the loss of lateral limb control was still significant after 15 months (Fig. 3E,F), although there was some improvement in the curvature at the starting point of the swing phases.

Differences in the swing phases in the X–Y plane before and after surgery were reflected in their dynamics. Limb velocity was determined in phase plane plots as a function of the change in position along the X-axis (Δx), which is the X-axis project of the swing length in space. The hindlimb and forelimb had similar dynamics along the X-axis before (Fig. 4A, hindlimb; Fig. 4C, forelimb) and after surgery (Fig. 4E,G), although, there was greater variation in the ending of the swing phases of both fore and hind limbs after surgery (Fig. 4E,G). This variation was probably caused by the diverging swing-phase directions after canal plugging, which shortened the swing length in space.

Dynamics along the Y-axis were much different. The phase plane plots along the Y-axis were coherent before surgery for both the hindlimbs and forelimbs (Fig. 4B,D), whereas after surgery, the Y-axis velocities were widely spread, more in the RFL than the RHL (Fig. 4F,H). The variance at the onset of the swing phases ($\Delta x = 0$ in Fig. 4H) was due to the fact that Y-axis velocities were already present at the onset of the swing phases and varied in direction and magnitude (Fig. 3C,D). These findings show that the canal plugging had produced a long-lasting lack of Y-axis (lateral) coordination of the swing phases, resulting in aberrant paw placements.

Discussion

These data demonstrate that the semicircular canals provide critical low- and mid-band frequency information through the aVCR and other vestibulo-spinal inputs to control head and limb movement during normal quadrupedal locomotion. The most dramatic change was in the accuracy and precision of lateral forelimb and hindlimb placement during the swing phases in the X–Y plane. Although the results presented here are from a single animal, a unique feature of the study was that we were able to follow an animal before and after all six canals were plugged, and compare the post-operative data to the normal preoperative findings, just after recovery, and a year later. The difficulty in lateral control of the fore and hind limbs during the swing phases and dispersion of the swing phases continued long after the initial surgery and was present more than a year after lesion. Thus, it appears to be a permanent deficit after canal plugging.

The paw placements after canal plugging had two characteristics. The gait was broad-based, so that the animals held the paws wider apart. This behavior was more prominent in the forelimbs, which steered the locomotion, than in the hindlimbs, which drove it.[15] In addition to holding its forelimbs and hindlimbs more laterally, there were broadened oval trajectories of the limbs during the swing phases, with a wide variation in direction in the X–Y plane (Fig 2D). There was also a significant Y-axis component just before the beginning of the swing phases that caused the final placement of the paws to be broadened. This type of behavior is consistent with the reported increased lack of lateral postural stability above that of fore–aft stability following unilateral vestibular lesions in humans.[4,5]

There has been considerable emphasis on the role of the otoliths in enhancing postural stability in static conditions,[16] and some damage of the otoliths cannot be totally discounted because of the proximity of the utricles to the canals that were plugged. However, low-frequency otolith control of balance appears to be primarily directed toward control of body sway and maintenance of the upright.[16] In addition, the effects of utricular damage on eye movements adapt rapidly after unilateral vestibular damage in humans.[17]

Electrical stimulation of individual canal nerves has demonstrated that continuous low-frequency (100 Hz) stimulation causes cats to have prolonged postural responses in the plane of the activated canal nerve.[18] Lateral canal nerve stimulation caused the head to turn to the contralateral side, associated with flexion of the contralateral forelimb and extension of the ipsilateral forelimb. If the stimulation continued, the animals circled in the plane of the lateral canals, making complete turns to the contralateral side with appropriate flexion and extension of the forelimbs. The hindlimbs supported the turning but were less involved. This showed that the lateral canals can regulate placement of the forepaws and heading of the body in the plane of the lateral canals.

The foot-placement responses following plugging of all canals complement these findings. Foot placement following canal plugging suggests that low- to mid-band frequency input from the semicircular canals contributes significantly to lateral postural stability and heading during active locomotion. The finding that splaying of paw placement was present long after

lesions further suggests that this function is not readily assumed by other systems as adaptation occurs during recovery.

Acknowledgments

NIH grants: EY11812, EY04148, DC-09255, DC02390, DC05204, EY01867

References

1. Gruneberg C, et al. Spatio-temporal separation of roll and pitch balance-correcting commands in humans. J Neurophysiol. 2005; 94:3143–3158. [PubMed: 16033938]
2. Carpenter MG, Allum JH, Honegger F. Vestibular influences on human postural control in combinations of pitch and roll planes reveal differences in spatiotemporal processing. Exp Brain Res. 2001; 140:95–111. [PubMed: 11500802]
3. Bauby CE, Kuo AD. Active control of lateral balance in human walking. J Biomech. 2000; 33:1433–1440. [PubMed: 10940402]
4. Mbongo F, et al. Postural control in patients with unilateral vestibular lesions is more impaired in the roll than in the pitch plane: a static and dynamic posturography study. Audiol Neurootol. 2005; 10:291–302. [PubMed: 15925864]
5. Allum JH, Ledin T. Recovery of vestibulo-ocular reflex-function in subjects with an acute unilateral peripheral vestibular deficit. J Vestib Res. 1999; 9:135–144. [PubMed: 10378185]
6. Ewald, JR. Physiologische Untersuchungen über das Endorgan des Nervus Octavus. J. F. Bergmann; Weisbaden: 1892.
7. Minor LB, Goldberg JM. Influence of static head position on the horizontal nystagmus evoked by caloric, rotational and optokinetic stimulation in the squirrel monkey. Exp Brain Res. 1990; 82:1–13. [PubMed: 2257895]
8. Yakushin SB, et al. Dynamics and kinematics of the angular vestibulo-ocular reflex in monkey: effects of canal plugging. J Neurophysiol. 1998; 80:3077–3099. [PubMed: 9862907]
9. Hess BJ, et al. Central versus peripheral origin of vestibuloocular reflex recovery following semicircular canal plugging in rhesus monkeys. J Neurophysiol. 2000; 84:3078–3082. [PubMed: 11110835]
10. Rabbitt R, et al. Influence of surgical plugging on horizontal semicircular canal mechanics and afferent response dynamics. J Neurophysiol. 1999; 82:1033–1053. [PubMed: 10444695]
11. Xiang Y, et al. Dynamics of quadrupedal locomotion of monkeys: implications for central control. Exp Brain Res. 2007; 177:551–572. [PubMed: 17006683]
12. Xiang Y, et al. Head Stabilization by Vestibulo-Collic Reflexes during Quadrupedal Locomotion in Monkey. J Neurophysiol. 2008; 100:763–780. [PubMed: 18562554]
13. Kunin M, et al. Rotation axes of the head during positioning, head shaking, and locomotion. J Neurophysiol. 2007; 98:3095–3108. [PubMed: 17898142]
14. Raphan T. Modeling control of eye orientation in three dimensions. I. Role of muscle pulleys in determining saccadic trajectory. J Neurophysiol. 1998; 79:2653–2667. [PubMed: 9582236]
15. Mori S, et al. Quadrupedal locomotor movements in monkeys (M. Fuscata) on a treadmill: kinematic analyses. Neuroreport. 1996; 7:2277–2285. [PubMed: 8951840]
16. Beule AG, Allum JH. Otolith function assessed with the subjective postural horizontal and standardised stance and gait tasks. Audiol Neurootol. 2006; 11:172–182. [PubMed: 16479089]
17. Kim HA, et al. Otolith dysfunction in vestibular neuritis: recovery pattern and a predictor of symptom recovery. Neurology. 2008; 70:449–453. [PubMed: 18250289]
18. Suzuki J, Cohen B. Head, eye, body and limb movements from semicircular canal nerve. Exp Neurol. 1964; 10:393–405. [PubMed: 14228399]

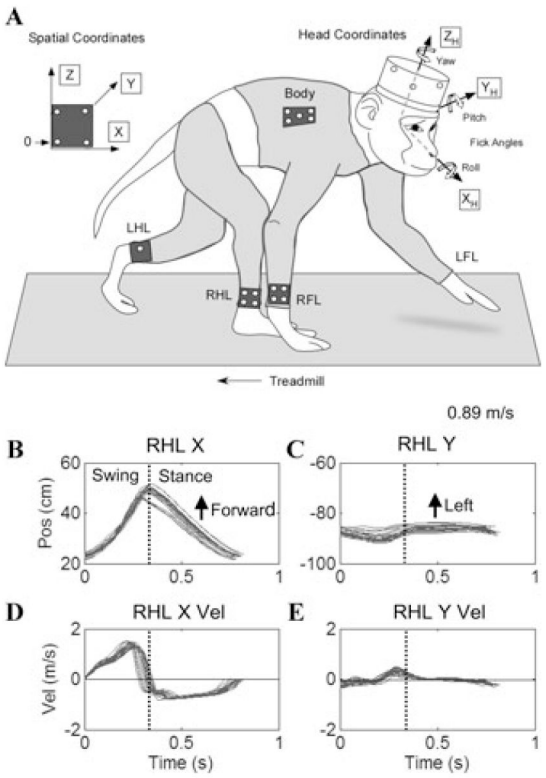

Figure 1.

Experimental configuration and normal gait in Cy115: (**A**) Coordinate frames and placement of rigid bodies on the head, chest, and limbs. The spatial reference rigid body is shown on the left. 0 is the origin. The X-axis in space is forward in the direction of walking, the Y-axis in space is to the animal's left, and the Z-axis in space is vertical. Head coordinates are marked as X_H, Y_H, Z_H, and the positive Fick angles are shown for yaw, pitch, and roll. LFL, left forelimb; RFL, right forelimb; LHL, left hindlimb; RHL, right hindlimb. (**B**, **C**) Position of the hindlimb along the X- and Y-axes as a function of time while walking at 0.89m/sec. The vertical dotted line shows the end of the swing phases and the beginning of the stance phases. The forward and lateral movements of the hindlimb are marked in **B** and **C. D, E,** X- and Y-axis velocities versus time. The inflection in the velocity during the swing phase in **D** is due to the multijoint movement. Movement of the hindlimb to the left or right of the Z-axis is reflected in velocities above or below the zero line. Note that there was very little lateral or medial deviation of the hindlimb in the pre-operative normal walking in **E**. (n = 19).

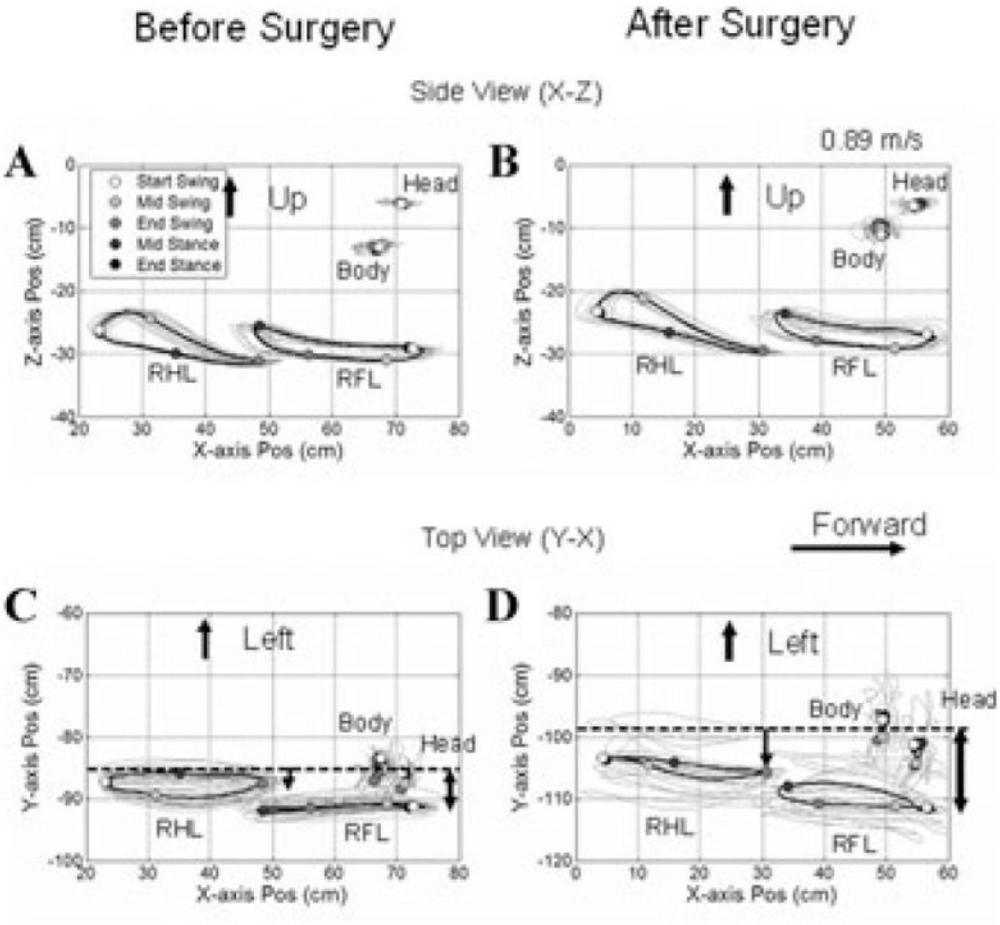

Figure 2.

Side (X–Z, **A, B**) and top (Y–X, **C, D**) views of Cy115's walking at 0.89 m/sec before (**A, C**) and 20 days (**B, D**) after all six semicircular canals were plugged. The ordinates in **A** and **B** show the Z position of the limb as a function of position along the X-axis. Open circles mark the beginning of the right hindlimb (RHL), and they become progressively darker as the RHL progresses from swing through stance phases. The head and body positions are also shown. The animal had its head turned slightly to the right as shown both in **C** and **D**. The limb movements were not changed in the X–Z projections before and after surgery (**A, B**), but there was considerable increase in the variation of the limb movements in the Y–Z plane (**D**) after canal plugging. The animal also had a broad-based gait, more in the forelimbs, as shown by the distance of the RFL from the body (**C, D**, arrows).

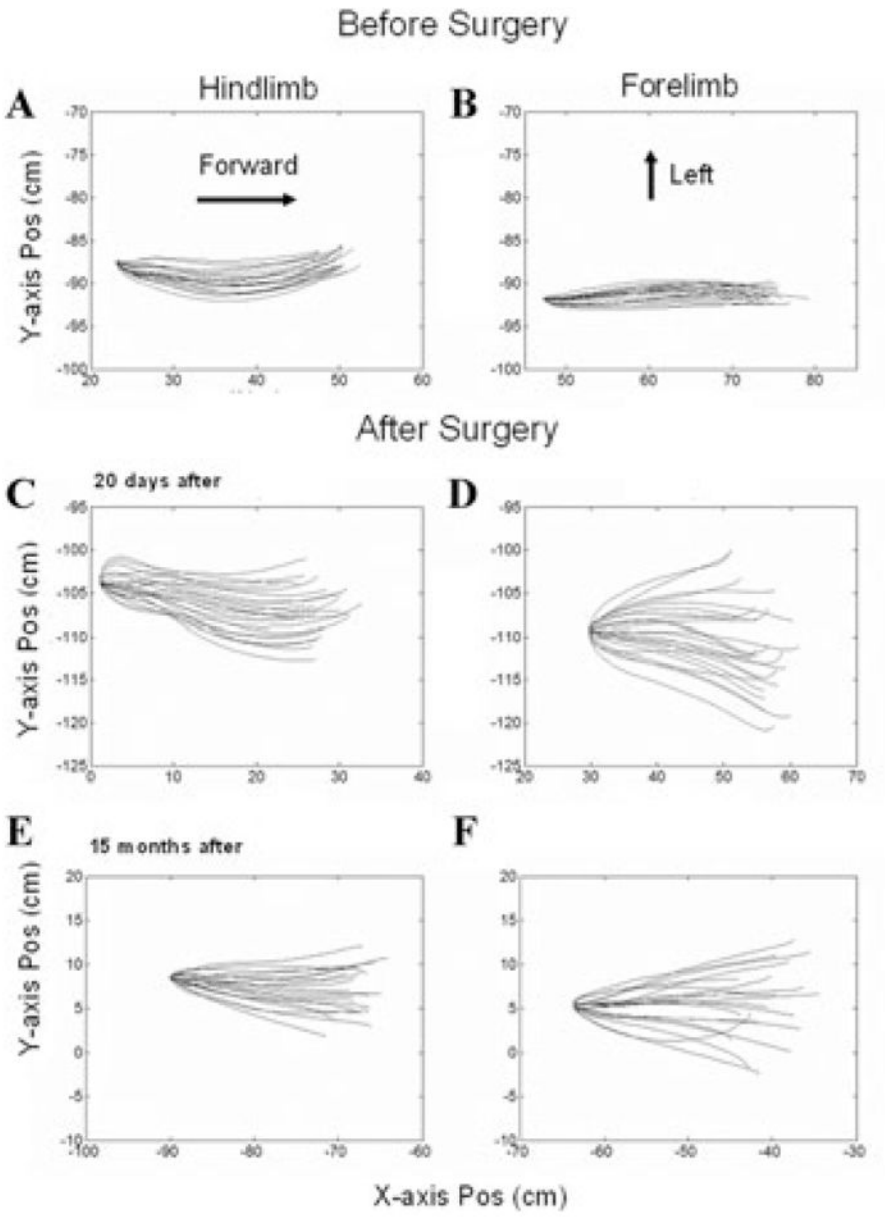

Figure 3.

Swing-phase trajectories of right hindlimb (**A, C, E**) and right forelimb (**B, D, F**) before (**A, B**), 20 days after (**C, D**), and 15 months after (**E, F**) all six semicircular canals were plugged. The swing phases were normalized to the same initial position, and the trajectories are displayed in the X–Y plane (*top view*). The displacement in the X direction is shown on the abscissae, and the Y direction on the ordinates. Note the marked splaying of the trajectories after surgery.

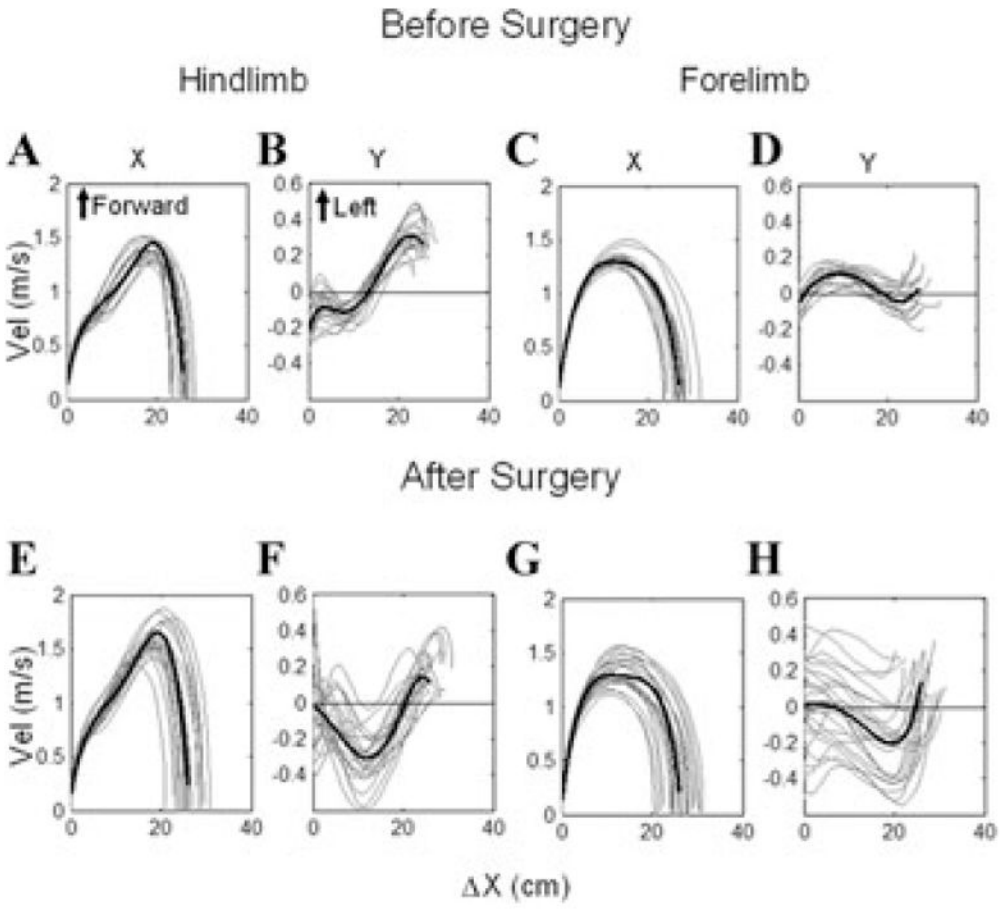

Figure 4.

Phase plane plots of the right hindlimb (**A, B, E, F**) and right forelimb (**C, D, G, H**) swing phase velocities (**C, D, G, H**) before (**A–D**) and after (**E–H**) all six semicircular canals were plugged. The position of the limbs along the X-axis is shown on the abscissae, plotted against the X-axis velocity in **A, C, E, G**, and against the Y-axis velocity of the limbs in **B, D, F, H**. Note the broadened endpoints of the swing-phase X-axis velocities in **E, G**, and the dispersion of the Y-axis velocities in **F, H** after the semicircular canals were plugged.

TABLE 1

Changes in Limb Kinematics

	RHL to Body Lateral Distance (cm) *P* = 0.105	RFL to Body Lateral Distance (cm) *P* < 0.001	RHL Swing Width (cm) *P* < 0.001	RFL Swing Width (cm) *P* < 0.001	RHL Swing Width Variation (cm) *P* < 0.001	RFL Swing Width Variation (cm) *P* < 0.001
Before (*n* = 14)	3.2 ± 1.0	7.3 ± 1.3	1.3 ± 0.4	1.5 ± 0.5	1.5 ± 0.6	1.8 ± 0.6
After (*n* = 14)	3.7 ± 0.9	11.7 ± 0.8	3.2 ± 0.6	3.4 ± 0.6	2.8 ± 0.7	3.5 ± 1.0

For the *P* values, seven matched speeds (0.63–0.89 m/sec) were used for a paired *t* test. Two experiments for “before” data (7 × 2 = 14, 10/28/05 and 11/03/05) and two experiments for “after” data (5/10/06 and 5/11/06).

TABLE 2

Changes in Peak-to-Peak Amplitudes of Head Movements

	Head X (cm) *P* = 0.006	**Head Y (cm) *P* = 0.0003**	**Head Z (cm) *P* = 0.0002**	**Head Yaw ° *P* = 0.34**	**Head Pitch ° *P* = 0.0044**	**Head Roll ° *P* < 0.001**
Before (*n* = 14)	1.1 ± 0.3	4.1 ± 0.8	0.5 ± 0.1	6.7 ± 5.7	3.6 ± 0.7	2.4 ± 0.7
After (*n* = 14)	1.5 ± 0.3	6.2 ± 1.6	1.1 ± 0.3	8.6 ± 4.0	5.7 ± 1.9	4.9 ± 1.3